Received: 1 September 2023 | Revised: 28 December 2023 | Accepted: 14 February 2024

IET Control Theory & Applications

DOI: 10.1049/cth2.12657

The Institution of Engineering and Technology WILEY

ORIGINAL RESEARCH

Intention inference-based interacting multiple model estimator in photoelectric tracking

Minxing Sun[1,2,3,4] | Huabo Liu[5] | Qianwen Duan[1,2,3,4] | Junzhe Wang[1,2,3,4] | Yao Mao[1,2,3,4] | Qiliang Bao[1,2,3,4]

[1]National Key Laboratory of Optical Field Manipulation Science and Technology, Chinese Academy of Science, Chengdu, Sichuan, China

[2]Key Laboratory of Optical Engineering, Chinese Academy of Sciences, Chengdu, Sichuan, China

[3]Institute of Optics and Electronics, Chinese Academy of Sciences, Chengdu, Sichuan, China

[4]School of Electronic, Electrical and Communication Engineering, University of Chinese Academy of Sciences, Beijing, China

[5]School of Automation, Qingdao University, Qingdao, Shandong, China

Correspondence
Yao Mao, National Key Laboratory of Optical Field Manipulation Science and Technology, Chinese Academy of Science, Chengdu 610209, Sichuan, China.
Email: maoyao@ioe.ac.cn

Funding information
National Natural Science Foundation of China, Grant/Award Number: 62271109

Abstract

Aiming to improve the estimation and prediction accuracy of a target's position, this paper proposes a state estimation method for photoelectric tracking systems, based on the evaluation of the tracked target's motion intention. Traditional photoelectric tracking systems utilize external physical quantities such as the position, velocity, and acceleration of the target as the estimated states. While this method can output good results for pre-modelled target positions, it struggles to maintain the accuracy when facing manoeuvering targets or complex motion patterns targets. Here, the relevant parameters of the tracked target's motion intention are directly estimated innovatively, like estimating the circling point position rather than the circular flying target's position and velocity. This approach enables recognizing the target's motion intention and leads to precise estimation, which specifically consists of an interacting multiple model approach, multiple unscented Kalman estimators, and a robust estimator. The effectiveness and stability of this estimator are validated through software simulations and experiments on a dual-reflection mirror platform.

1 | INTRODUCTION

The optoelectronic tracking system finds widespread applications in target tracking [1, 2], optical communication [3, 4], and medical surgery [5]. It mainly consists of signal acquisition [6], image processing [7], position estimation [8–10], and a gimbal-control system [11, 12]. Optoelectronic tracking systems face various challenges. For instance, time constraints in optical imaging and image processing can result in significant system delays. Moreover, non-uniform optical path media and camera imaging quality can introduce observation noise [13, 14]. To achieve fast and precise target tracking, it becomes crucial to employ state estimation algorithms to mitigate the impact of noise, accurately estimating the state information of the tracked target, and predicting the target's position to compensate for camera delays.

The origins of state estimation algorithms can be traced back to the early 19th century with the development of least squares estimation methods for computing celestial orbit trajectories [15]. In the 1960s, the introduction of Wiener filter and Kalman filter laid the foundation of state estimation methods [16, 17]. However, these methods had various limitations such as relying on the autocorrelation function of signals and precise linear state space equations. To address these challenges, new state estimation methods were further explored and applied. Zames utilized the H_∞ concept to design the H_∞ estimation method, which achieved robustness against predetermined motion model errors and noise model errors [18, 19]. Various improvements to the Kalman filtering method had also compensated for model uncertainties [20–22]. Unscented Kalman filter, ensemble Kalman filtering, and other methods had extended the applicability of the Kalman filtering method

to non-linear state space models [23–25]. Modern data-driven methods such as support vector machines [26], recurrent neural networks [27], and causality representation theory [28] had further enriched the toolkit of state estimation.

However, the application of photoelectric tracking systems often involves manoeuverable or even non-cooperative aircraft as tracked targets. This necessitates that estimation algorithms maintain their capabilities when dealing with targets exhibiting hybrid motion trajectories. One such method is the multiple model particle filter. By combining sequential importance sampling and Markov chain Monte Carlo methods [29, 30], this approach aims to achieve optimal estimation, albeit with higher computational costs. The static multiple model estimator is one other method that utilizes Bayesian rules to estimate the weights of several possible motion models and combines their results through weighted summation to obtain the final estimation value [31]. The interacting multiple model (IMM) method is another crucial approach. This method uniquely calculates the likelihood of a specific model by weighing both its estimation accuracy and the preset probabilities of transitioning from other models [32, 33]. This dual consideration enables the integration of extensive prior knowledge about motion patterns, significantly enhancing estimation accuracy. Leveraging IMM's strengths, researchers have advanced the field with developments like optimized sub-estimator selection [34, 35], faster model-switching methods [36], and improved methods for assessing estimation performance [37].

In our research, we identified that most state estimation algorithms currently employed in photoelectric tracking systems rely on the external physical features of the tracked target as the estimated states, that is, position, velocity, and acceleration [38]. This prevailing approach may have been inherited from the classical control theory's use of state values and their higher-order differentials [39]. Furthermore, the integration of other components in the gimbal control loop, which utilize position and velocity, also likely reinforces this traditional method [40]. In reality, the state estimation algorithm operates based on the motion model of the tracked target and is independent of the parameters and controls of the tracking device. It forms a separate system. Upon realizing this, this paper innovatively explores alternative methods for setting the estimated states. For example, when the tracked target is circling in the air, instead of using its position, velocity, and acceleration as the estimated states, we estimate its circling point coordinates and employ robust state estimation, unscented Kalman estimator (UKE), and modified IMM methods to construct the intention inference-based interacting multiple model estimator (IIIMME). This represents a fundamental shift from estimating the external physical parameters of the tracked target to estimating the intention-related parameters of the target.

When dealing with tracked targets exhibiting hybrid motion, the intent inference-based estimation method can offer several advantages: (1) It significantly improves estimation accuracy and prediction effectiveness. (2) It effectively mitigates the impact of observation noise. (3) It shows potential for long-term prediction in occlusion scenarios. Implementing this new method could lead to remarkable accuracy improvements in the prediction component, and it may even enhance the performance of optoelectronic tracking systems.

The subsequent sections of this paper are organized as follows: Section 2 introduces the design method for the new state estimation quantity. In Section 3, The algorithm of modified IMM is demonstrated. In Section 4, the state space model and algorithm of the UKE are described. Section 5 discusses the state space model and computational methods of the robust state estimator. The effectiveness of the proposed IIIMME algorithm is evaluated through simulations and experiments in Section 6. Finally, Section 7 provides the conclusion of the research.

2 | DESIGN METHOD OF ESTIMATED STATES

2.1 | State space model

The motion of the tracked target in photoelectric tracking systems is commonly described using the following general linear state space model:

$$\begin{aligned} x_{k+1} &= F_k x_k + G_k w_k \\ z_k &= H_k x_k + u_k. \end{aligned} \tag{1}$$

where x_k and z_k represent the state parameters and observation results of the tracked target at time k, respectively. The state parameters x_k are typically set as the position of the tracked target and its relevant differentials such as velocity and acceleration. However, in this study, we propose a shift from these traditional kinematic states to parameters that better capture the motion intention of the tracked target. The type of observation z_k depends on the operational principles of the tracking device, with the device's output typically being the position value of the tracked target. The initial value of the tracked target's position x_0, process noise w_k, and observation noise u_k follows Gaussian distributions.

$E(\cdot)$ represents the expectation, and δ_{ij} is the Kronecker symbol equation, while $i = j$, $\delta_{ij} = 1$; $\delta_{ij} = 0$ if $i \neq j$ satisfied. In the application of photoelectric tracking systems, the covariance matrices for process noise Q_i and observation noise R_i should be set based on the unmanned aerial vehicle's flight environment and the performance of the observation device. These matrices are typically treated as constants (2).

$$\mathrm{E}\left(\begin{bmatrix} x_0 \\ w_i \\ u_i \end{bmatrix}\begin{bmatrix} x_0 \\ w_j \\ u_j \end{bmatrix}^T\right) = \begin{bmatrix} \Pi_0 & & \\ & Q_i\delta_{ij} & \\ & & R_i\delta_{ij} \end{bmatrix} \tag{2}$$

In the state space model (1), F_k represents the state transition matrix, G_k is the process noise driving matrix, and H_k is the state observation matrix. They are typically set as constant matrices and have a generic numerical form. When the observed

outputs of the tracked target are the position values in the X and Y axes, denoted as $O_{x,k}$ and $O_{y,k}$, respectively, and the estimated states consist of the positions $p_{x,k}$ and $p_{y,k}$, as well as the velocities $v_{x,k}$ and vy, k in the two axes, the state space model is as follows:

$$\begin{bmatrix} p_{x,k+1} \\ v_{x,k+1} \\ p_{y,k+1} \\ v_{y,k+1} \end{bmatrix} = \begin{bmatrix} 1 & S & 0 & 0 \\ 0 & 1 & 0 & 0 \\ 0 & 0 & 1 & S \\ 0 & 0 & 0 & 1 \end{bmatrix} \begin{bmatrix} p_{x,k} \\ v_{x,k} \\ p_{y,k} \\ v_{y,k} \end{bmatrix} + w_k$$

$$\begin{bmatrix} O_{x,k} \\ O_{y,k} \end{bmatrix} = \begin{bmatrix} 1 & 0 & 1 & 0 \end{bmatrix} \cdot \begin{bmatrix} p_{x,k} & v_{x,k} & p_{y,k} & v_{y,k} \end{bmatrix}^T + u_k. \quad (3)$$

The parameter S in the model represents the sampling period of the optical sensor, which is a simple constant velocity motion model. Due to the omission of many factors, both the estimation accuracy and prediction accuracy of the algorithm will significantly decrease. This trade-off is often made when dealing with manoeuvering targets using traditional state estimation methods. This study aims to improve this by introducing a new approach to setting the estimated states.

2.2 | Design rule for estimated states

From an engineering perspective, achieving IIIMME requires several steps. First, a large amount of trajectory data needs to be collected. Then, the data is clustered, function fitted, and represented according to different intentions. Finally, the IIIMME is implemented. Here, the focus will be on the setting of the estimated states and the relevant estimation algorithms. Regarding how to set the estimated states, the following simple example will illustrate the viewpoint.

In the case where the tracked target is undergoing one-dimensional sinusoidal motion with position $p = A \sin \omega t$, let us assume that the photoelectric tracking system is aware of this motion pattern and need not use the general state space model described in (1). Traditional state estimation methods consider the position p and velocity v of the tracked target as the estimated states. When the sampling interval S of the system and the angular velocity ω of the sinusoidal motion are accurately known, the initial state $[p_0 \quad v_0]^T$ is correctly set (implicitly including the amplitude of the sinusoidal motion), and the following linear state space equations can be derived for state estimation and position prediction (4):

$$\begin{bmatrix} \mathrm{p}_{k+1} \\ v_{k+1} \end{bmatrix} = \begin{bmatrix} A \sin(\omega t + \omega \mathrm{S}) \\ A\omega \cos(\omega t + \omega \mathrm{S}) \end{bmatrix} = \begin{bmatrix} \cos(\omega \mathrm{S}) & \frac{\sin(\omega \mathrm{S})}{\omega} \\ -\omega \sin(\omega \mathrm{S}) & \cos(\omega \mathrm{S}) \end{bmatrix} \begin{bmatrix} \mathrm{p}_k \\ v_k \end{bmatrix}. \quad (4)$$

However, in practical applications, it is nearly impossible to accurately predefine the initial state $[p_0 \quad v_0]^T$ before the start of the estimation process. The angular velocity ω and amplitude A of the tracked target's sinusoidal motion may also vary. This makes it challenging to achieve accurate position estimation and prediction.

To address this issue, this study attempts to use intention-related parameters instead of the external physical quantities of the tracked target as the estimated states. Analyzing the model reveals that the main parameters of this motion pattern include the amplitude A, angular velocity ω (replaced by a more general periodic time parameter, denoted as T), and a current time parameter t. The following state space model can be established (5):

$$x_{k+1} = \begin{bmatrix} t_{k+1} \\ T_{k+1} \\ A_{k+1} \end{bmatrix} = x_k + \begin{bmatrix} S \\ 0 \\ 0 \end{bmatrix} + w_k$$

$$z_k = A_k \sin\left(\frac{2\pi}{T_k} t_k\right) + u_k. \quad (5)$$

The advantages of this new approach are as follows:

1. It relies less on predefined initial values, and accurate estimation can be achieved more quickly by estimating the current time parameter t.
2. This new approach successfully estimates amplitude and period without the need for precise preset values. Although this model is also limited to estimating targets that exhibit sinusoidal motion, it demonstrates significantly improved adaptability compared to the traditional state space equation (4) that can only estimate specific sinusoidal motion. The traditional model is restricted to estimating sinusoidal motion with specific amplitudes, dependent on accurate initial value settings and angular velocities that require precise ω settings as outlined in (4).
3. The estimated states of amplitude and period typically remain constant or change slowly. As the number of motion cycles of the tracked target increases, these parameters gradually converge to their accurate true values. This is not only beneficial for accurate state estimation but also enables long-term position prediction and resistance to observation noise and target occlusion.

The name "intention-related parameters" is employed due to their proximity to the operator's intentions in manoeuvering target control. Using the illustrative model, a widely adopted sinusoidal input signal in research experiments, researchers predominantly focus on the amplitude and frequency of the wave, rather than the precise variations in position and velocity. Then, directly estimating the relatively stable and approximately constant intention parameters enhances estimation accuracy.

It is worth noting that for target tracking tasks with periodic characteristics, a more general form of the state transition

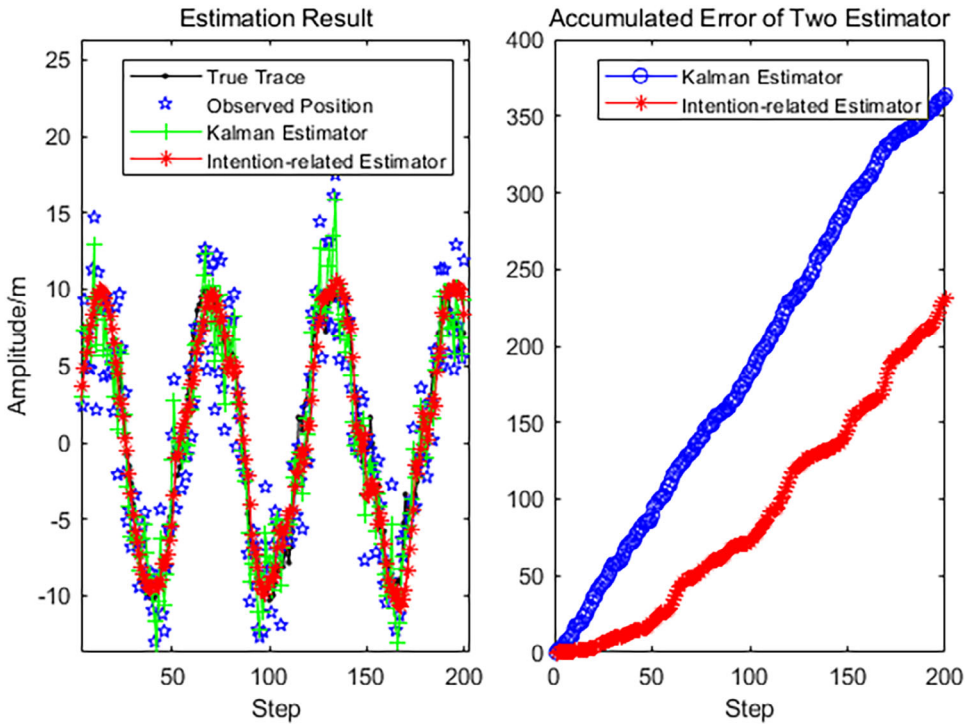

FIGURE 1 The simulated true trace and estimation result.

equation can be provided as (6):

$$\varkappa_{k+1} = \varkappa_k + \begin{bmatrix} \mathcal{S} \\ 0 \\ 0 \\ \vdots \\ 0 \end{bmatrix} = \begin{bmatrix} t_k \\ T \\ c_1 \\ \vdots \\ c_n \end{bmatrix} + \begin{bmatrix} \mathcal{S} \\ 0 \\ 0 \\ \vdots \\ 0 \end{bmatrix}, \tag{6}$$

where time t and periodic time T are the estimated states that are common to all periodic motions. The parameters $c_1, c_2, \ldots, c_n$ represent the specific parameters for different motion patterns. For example, in the case of sinusoidal motion, the specific parameter amplitude A can be considered as c_1.

Figure 1 is an estimation accuracy comparison between the traditional Kalman estimator (designed based on (4) and accurate initial state) and the new intention-related estimator in the case of sinusoidal motion (5). The accumulative error between the true value and the estimated value of state $\varkappa$ is also depicted in the figure. This comparison briefly demonstrates the advantages of the new design method, and more simulation experiments will be presented in Section 6. Through the simulations, it can be observed that the new method significantly improves the estimation accuracy.

3 | THE ALGORITHM OF MODIFIED IMM

After setting the states for a single motion intention, in practical applications, it is necessary to integrate and assess multiple motion intention estimators to achieve intent inference and accurate estimation. Here, we utilize the modified IMM method to accomplish this process, as its interactive mechanism holds significant practical relevance in intention inference. Here, we present a hypothesis for demonstrating: When the tracked target has already made a 30-degree left turn, the likelihood of the target continuing to turn left in the next time step is higher than the likelihood of it going straight and much higher than turning right. In this case, the IMM method can improve the estimation performance of the estimator by statistically analyzing and predetermining the state transition probabilities between different intentions.

The specific implementation of the modified IMM algorithm involves four steps, and the algorithm is as follows:

- **Initialization.**

  This step requires pre-setting based on the learning results from the motion trajectory dataset and the application scenario of target tracking. Specifically, it includes the initial value $\hat{X}_0$ of the position estimate for the tracked target, the probability transition matrix Γ for different intentions of the tracked target, the probability μ_s for each current motion intention of the tracked target, the specific form of the r individual intention state estimators E_s, the initial state estimation $\hat{x}_{s,0}$ of the estimator E_s, and the initial covariance $\hat{P}_{s,0}$ of the posterior estimation error.

  It should be noted that the elements Γ_{ij} in the probability transition matrix Γ represent the probability of the tracked target transitioning from intention i to intention j (7):

$$\Gamma = \begin{bmatrix} \Gamma_{11} & \cdots & \Gamma_{1r} \\ \cdots & \cdots & \cdots \\ \Gamma_{r1} & \cdots & \Gamma_{rr} \end{bmatrix}. \tag{7}$$

- **Intention estimators E_s separately estimating.**

  In traditional interacting multiple model estimation methods, the second step involves input interacting, where the estimation results of E_s are adjusted based on the results of estimators other than E_s. This is based on the assumption that different sub-estimators have compatible estimated states. However, intention estimators have independent forms of the estimated states, with different dimensions and physical interpretations, making the input interaction among different intention estimators meaningless.

  Therefore, here, the input interaction step is removed, and each intention estimator directly estimates based on the observed values z_k and predetermined parameters within the algorithm. The specific algorithm design for the intention estimators will be discussed in the following two sections. The output of the estimator E_s includes the position estimation value $\hat{z}_{s,k}$ and the position estimation covariance $\hat{S}_{s,k}$.

- **Intention probability evaluation.**

  After obtaining the position prediction results $\hat{z}_{s,k}$ from each specific intention state estimator, the interacting algorithm needs to evaluate the probabilities μ_s of the current motion intentions of the tracked target. The calculation method is as (8):

$$\begin{aligned}
\mu_{s,k} &= \Lambda_{s,k}\bar{c}_s / c \\
c &= \sum_{s=1}^{r} \Lambda_{s,k}\bar{c}_s \\
\Lambda_{s,k} &= \frac{1}{(2\pi)^{n/2}\left|\hat{S}_{s,k}\right|^{1/2}} \exp\left\{-\frac{v_{s,k}^T \hat{S}_{s,k}^{-1} v_{s,k}}{2}\right\} \\
v_{s,k} &= z_k - \hat{z}_{s,k} \\
\bar{c}_s &= \sum_{i=1}^{r} \Gamma_{i,s}\mu_{s,k-1}.
\end{aligned} \tag{8}$$

  In the above formula, $v_{s,k}$ represents the estimation error of the target position, $\Lambda_{s,k}$ is the likelihood function of intention s, $\bar{c}_s$ is the probability of intention s, and c is the normalization constant.

- **Output interaction.**

  The final step of the intention-based interacting multiple model state estimator is to weigh the target position estimation results from the specific intention state estimators. The calculation is based on the probabilities $\mu_{s,k}$ and outputs the target position prediction value $\hat{z}_k$ of the entire estimator (9):

$$\begin{aligned}
\hat{z}_k &= \sum_{s=1}^{r} \hat{z}_{s,k}\mu_{s,k} \\
\hat{P}_{k|k} &= \sum_{s=1}^{r} \mu_{s,k}\{\hat{S}_{s,k} + [\hat{z}_{s,k} - \hat{z}_k] \cdot [\hat{z}_{s,k} - \hat{z}_k]^T\}.
\end{aligned} \tag{9}$$

  After obtaining new observed values $\hat{z}_k$ of the tracked target, the estimator needs to return to step 2 for a new estimation iteration.

4 | THE ALGORITHM OF UKE

The design of the intention estimators in this study is based on the classical UKE method. This method extends the Kalman filtering approach to the field of non-linear estimation through the use of the unscented transform (UT). The specific calculation steps are as follows:

The state space equation corresponding to the specific intention state estimator needs to be derived based on the trajectory data:

$$\begin{aligned}
x_{s,k+1} &= f_s(x_{s,k}, w_{s,k}) \\
z_{s,k} &= h_s(x_{s,k}, u_{s,k}),
\end{aligned} \tag{10}$$

where $x_{s,k}$ and $z_{s,k}$ represent the state and observation values of the specific intention state estimator in the interacting state estimator for intention s, respectively. $f_s(x_{s,k}, w_{s,k})$ and $h_s(x_{s,k}, u_{s,k})$ denote the state transition and observation equations for intention s, respectively. The variables $x_{s,0}$, $w_{s,k}$, and $u_{s,k}$ follow a Gaussian distribution and satisfy the following properties:

$$\mathrm{E}\left(\begin{bmatrix} x_{s,0} \\ w_{s,k} \\ u_{s,k} \end{bmatrix}\begin{bmatrix} x_{s,0} \\ w_{s,k} \\ u_{s,k} \end{bmatrix}^T\right) = \begin{bmatrix} \Pi_0 & & \\ & Q_s\delta_{ij} & \\ & & R_s\delta_{ij} \end{bmatrix}. \tag{11}$$

The ideal extraction of intention parameters should ensure that the estimated state remains constant or changes with a deterministic step size when the tracked target's motion intention remains unchanged. This allows the state transition equation $f_s(x_{s,k}, w_{s,k})$ to be expressed in a linear form as (12):

$$\begin{aligned}
x_{s,k+1} &= \begin{bmatrix} 1 & 0 & 0 \\ 0 & \ddots & 0 \\ 0 & 0 & 1 \end{bmatrix} x_s + D \\
&= \begin{bmatrix} 1 & 0 & 0 \\ 0 & \ddots & 0 \\ 0 & 0 & 1 \end{bmatrix}\begin{bmatrix} c_1 \\ \vdots \\ c_n \end{bmatrix} + \begin{bmatrix} D_1 \\ \vdots \\ D_n \end{bmatrix},
\end{aligned} \tag{12}$$

where D_n is a constant that can be 0. The observation equation $h_s(x_{s,k}, v_{s,k})$ should be constructed based on reasonable intention parameters. Next, the estimation should be performed according to the following steps:

- Set the parameters α, β, κ, initial estimated state value $x_{s,0}$, initial covariance of the posterior estimation error $\hat{P}_{s,0}$,

observation noise covariance R_s, and process noise covariance Q_s based on the target tracking scenario;
- Calculate the parameter λ based on the given value of α, κ and the dimension n of the estimated state $\hat{x}_{s,k|k-1}$:

$$\lambda = \alpha^2(n+\kappa) - n; \tag{13}$$

- Compute $2n+1$ Sigma points $X^{(l)}$ based on the estimated state $\hat{x}_{s,k|k-1}$, its dimension n, the precalculated values α, β, κ, and the covariance of the posterior estimation error $\hat{P}_{s,k-1}$, $((\sqrt{A})_i$ representing the square root of matrix A for the i-th column):

$$X^{(l)} = \begin{cases} X^{(0)} = \bar{X} & l = 0 \\ X^{(l)} = \bar{X} + \left(\sqrt{(n+\lambda)\hat{P}_{s,k-1}}\right)_l & l = 1 \sim n \\ X^{(l)} = \bar{X} - \left(\sqrt{(n+\lambda)\hat{P}_{s,k-1}}\right)_l & l = n+1 \sim 2n \end{cases}; \tag{14}$$

- Calculate the weights $w^{(l)}$ for each of the $2n+1$ Sigma points $X^{(l)}$:

$$w^{(l)} = \frac{\lambda}{2(n+\lambda)}, \quad l = 1 \sim 2n; \tag{15}$$

- Perform a one-step prediction to the $2n+1$ Sigma points $X^{(l)}$ by using the state transition equation $f_s(\cdot)$ to obtain $\hat{X}^{(l)} = f_s(X^{(l)})$;
- Calculate the prior state value $\hat{x}_{s,k|k-1}$ and covariance of the prior estimation error $\hat{P}_{s,k|k-1}$ for the estimated state x based on the $2n+1$ points $\hat{X}^{(l)}$ and their corresponding weights $w^{(l)}$:

$$\begin{aligned} \hat{x}_{s,k|k-1} &= \sum_{l=0}^{2n} w^{(l)} \hat{X}^{(l)} \\ \hat{P}_{s,k|k-1} &= \sum_{l=0}^{2n} w^{(l)} [\hat{x}_{s,k|k-1} - \hat{X}^{(l)}][\hat{x}_{s,k|k-1} - \hat{X}^{(l)}]^T + Q_s; \end{aligned} \tag{16}$$

- Apply the UT transform to the prior state value $\hat{x}_{s,k|k-1}$ to obtain $2n+1$ new Sigma points $\tilde{X}^{(l)}$:

$$\tilde{X}^{(l)} = \begin{cases} \tilde{X}^{(0)} = \hat{x}_{s,k|k-1}, & S1; \\ \tilde{X}^{(l)} = \hat{x}_{s,k|k-1} + \left(\sqrt{(n+\lambda)\hat{P}_{s,k|k-1}}\right)_l, & S2; \\ \tilde{X}^{(l)} = \hat{x}_{s,k|k-1} - \left(\sqrt{(n+\lambda)\hat{P}_{s,k|k-1}}\right)_l, & S3; \end{cases}$$

$$S1: l = 0; S2: l = 1 \sim n; S3 = l = n+1 \sim 2n \tag{17}$$

- Perform observation simulation for the $2n+1$ Sigma points $\tilde{X}^{(l)}$ based on the observation equation $h_s(\cdot)$ to obtain

$$Z^{(l)} = h_s(\tilde{X}^{(l)}); \tag{18}$$

- Predict the observation value $\tilde{Z}$ and covariance $P_{x\tilde{z}}$ and P_{zz} based on the $2n+1$ points $Z^{(l)}$ and their corresponding weights $w^{(l)}$

$$\begin{aligned} \tilde{Z} &= \sum_{l=0}^{2n} w^{(l)} Z^{(l)} \\ P_{\tilde{z}\tilde{z}} &= \sum_{l=0}^{2n} w^{(l)} [\tilde{Z} - Z^{(l)}][\tilde{Z} - Z^{(l)}]^T + R_s \\ P_{x\tilde{z}} &= \sum_{l=0}^{2n} w^{(l)} [\tilde{Z} - \tilde{X}^{(l)}][\tilde{Z} - Z^{(l)}]^T; \end{aligned} \tag{19}$$

- Calculate the Kalman gain matrix $K = P_{x\tilde{z}} P_{\tilde{z}\tilde{z}}^{-1}$;
- Calculate the estimation results $\hat{x}_{s,k}$ and covariance $\hat{P}_{s,k}$ for the specific intention state estimator E_s:

$$\begin{aligned} \hat{x}_{s,k} &= \hat{x}_{s,k|k-1} + K\left(z_k - \tilde{Z}\right) \\ \hat{P}_{s,k} &= \hat{P}_{s,k|k-1} - K P_{\tilde{z}\tilde{z}} K^T; \end{aligned} \tag{20}$$

- Calculate the estimated position value $\hat{z}_{s,k}$ for the tracked target based on the estimation result $\hat{x}_{s,k}$. Utilize the covariance propagation method for non-linear functions to calculate the position estimation error covariance $\hat{S}_{s,k}$. Here, $\hat{x}_{s,k}(n)$ represents the nth element of vector $\hat{x}_{s,k}$:

$$\begin{aligned} \hat{\tilde{z}}_{s,k} &= h_p(\hat{x}_{s,k}) \\ \hat{S}_{s,k} &= \left[\frac{\partial h_s(\hat{x}_{s,k})}{\partial \hat{x}_{s,k}(1)} \quad \frac{\partial h_s(\hat{x}_{s,k})}{\partial \hat{x}_{s,k}(2)} \quad \cdots \quad \frac{\partial h_s(\hat{x}_{s,k})}{\partial \hat{x}_{s,k}(n)}\right] \hat{P}_{s,k} \\ &\quad \left[\frac{\partial h_s(\hat{x}_{p,k})}{\partial \hat{x}_{s,k}(1)} \quad \frac{\partial h_s(\hat{x}_{s,k})}{\partial \hat{x}_{s,k}(2)} \quad \cdots \quad \frac{\partial h_s(\hat{x}_{s,k})}{\partial \hat{x}_{s,k}(n)}\right]^T. \end{aligned} \tag{21}$$

The above describes the design method of the UKE based on intention states. However, it is not sufficient to construct all sub-estimators using this method alone.

5 | THE ALGORITHM OF ROBUST ESTIMATOR

The intention estimator is learned based on trajectory data clustering. In practical applications, we cannot guarantee that the trajectory database includes all possible manoeuvering modes of the tracked target. Therefore, it is necessary to supplement a general state estimation method to improve the robustness of the system. Considering the non-linearity and manoeuverability

of the target's motion, linear equations of the form (1) cannot achieve accurate estimation. Here, we choose to use a robust state estimator for the general estimation [20], which is based on the state space equations (22):

$$\begin{aligned} x_{k+1} &= (F_k + \delta F_k)x_k + (G_k + \delta G_k)w_k \\ z_k &= H_k x_k + u_k \\ \begin{bmatrix}\delta F_k & \delta G_k\end{bmatrix} &= M_k \Delta_k [E_{f,k} \quad E_{g,k}]. \end{aligned} \tag{22}$$

Unlike equation (1), this equation incorporates the uncertainty terms δF_k and δG_k, which represent the errors between the true state transition equation parameters and the assumed state transition equation parameters. It further utilizes the time-varying matrix M_k; the scaling parameter Δ_k that takes values in the range of [0,1]; the expected values $E_{f,k}$ and $E_{g,k}$ of the model uncertainties, who decompose the uncertainty components together.

In the specific algorithm implementation, it utilizes an optimization parameter $\hat{\lambda}$ to timely adjust the parameters of the assumed model to adapt to the uncertainties. The calculation method of $\hat{\lambda}$ are as (23) and (24):

$$\begin{aligned} &\min_{\{x_j(k),w_j(k)\}} \max_{\{\delta F_j(k),\delta G_j(k)\}} E_1 + E_2 + E_3 \\ &E_1 = \left\| x_j(k) - \hat{x}_j(k) \right\|^2_{\hat{P}_j^{-1}(k)} \\ &E_2 = \left\| w_j(k) \right\|^2_{Q_j^{-1}(k)} \\ &E_3 = \left\| y_j(k+1) - H_j(k+1)x_j(k+1) \right\|^2_{R_j^{-1}(k+1)}. \end{aligned} \tag{23}$$

$$\begin{aligned} x &\leftarrow col\{x_j(k) - \hat{x}_j(k)\} \\ b &\leftarrow y_j(k+1) - H_j(k+1)x_j(k+1) \\ A &\leftarrow H_j(k+1)\begin{bmatrix}F_j(k) & G_j(k)\end{bmatrix} \\ \delta A &\leftarrow H_j(k+1)M_j\Delta_j\begin{bmatrix}E_{f,j}(k) & E_{g,j}(k)\end{bmatrix} \\ \delta b &\leftarrow -H_j(k+1)M_j\Delta_j E_{f,j}(k)\hat{x}_j(k) \\ Q &\leftarrow (\hat{P}_j(k)^{-1} \oplus Q_j(k)^{-1}) \\ W &\leftarrow R_j(k)^{-1} \\ H &\leftarrow H_j(k+1)M_j \\ E_a &\leftarrow \begin{bmatrix}E_{f,j}(k) & E_{g,j}(k)\end{bmatrix} \\ E_b &\leftarrow -E_{f,j}(k)\hat{x}_j(k) \\ \Delta &\leftarrow \Delta_i. \end{aligned} \tag{24}$$

Once the optimization parameter $\hat{\lambda}$ is obtained, the adjustment of process noise Q_{k-1}, observation noise R_k, state transition matrix F_{k-1}, and noise driving matrix G_{k-1} can be performed according to the following formulas:

$$\begin{aligned} \hat{Q}_{k-1}^{-1} &= Q_{k-1}^{-1} + \hat{\lambda}E_{f,k-1}^T \\ &\quad \cdot [I + \hat{\lambda}E_{f,k-1}P_{k-1|k-1}E_{f,k-1}^T]^{-1}E_{g,k-1} \\ \hat{R}_k &= R_k - \hat{\lambda}^{-1}H_{k-1}MM^T H_{k-1}^T \\ \hat{G}_{k-1} &= G_{k-1} - \hat{\lambda}F_{k-1}P_{k-1|k-1}E_{f,k-1}^T E_{g,k-1} \\ \hat{F}_{k-1} &= (F_{k-1} - \hat{\lambda}\hat{G}_{k-1}\hat{Q}_{k-1}E_{g,k-1}^T E_{f,k-1}) \\ &\quad \cdot (I - \hat{\lambda}P_{k-1|k-1}E_{f,k-1}^T E_{f,k-1}). \end{aligned} \tag{25}$$

Then, the robust state estimation can be performed using the adjusted parameters:

$$\begin{aligned} \hat{x}_{k|k} &= \hat{F}_{k-1}\hat{x}_{k-1|k-1} + P_{k|k}H_k^T\hat{R}_k^{-1} \\ &\quad \cdot (z_k - H_k\hat{F}_{k-1}\hat{x}_{k-1|k-1}) \\ P_{k|k} &= P_k - P_k H_k^T R_{e,k}^{-1} H_k P_k \\ P_k &= F_{k-1}\hat{P}_{k-1|k-1}F_{k-1}^T + \hat{G}_k\hat{Q}_k\hat{G}_k^T \\ \hat{P}_{k-1|k-1} &= (P_{k-1|k-1}^{-1} + \hat{\lambda}E_{f,k-1}^T E_{f,k-1})^{-1} \\ R_{e,k} &= \hat{R}_k + H_k P_k H_k^T. \end{aligned} \tag{26}$$

As part of IIIMME, the position $\hat{z}_{p,k}$ of the tracked target is estimated, and the covariance $\hat{S}_{p,k}$ of the position estimation error is calculated:

$$\begin{aligned} \hat{z}_{p,k} &= H_k\hat{x}_{k|k} \\ \hat{S}_{p,k} &= \hat{R}_k + H_k P_{k|k} H_k^T. \end{aligned} \tag{27}$$

6 | SIMULATION AND EXPERIMENT

The aforementioned algorithms constitute a complete IIIMME. In this section, the effectiveness and stability of the estimator will be verified through C programming simulations and experiments on a dual-reflector mirror platform.

6.1 | Simulation

In the C programming state estimation simulation, it is assumed that the tracked target has three motion intents: uniform linear motion, variable elliptical motion, and composite variable triangular wave motion (variable sawtooth wave motion) along the X and Y axes. Their motion trajectories are shown in Figure 2, with the target performing variable sawtooth wave motion M_1, followed by linear motion M_2, variable elliptical wave motion M_3, and finally linear motion M_4.

The motion model M_1 follows a triangular wave pattern along the x-axis and y-axis with a frequency $F_{M1} = 1$ Hz,

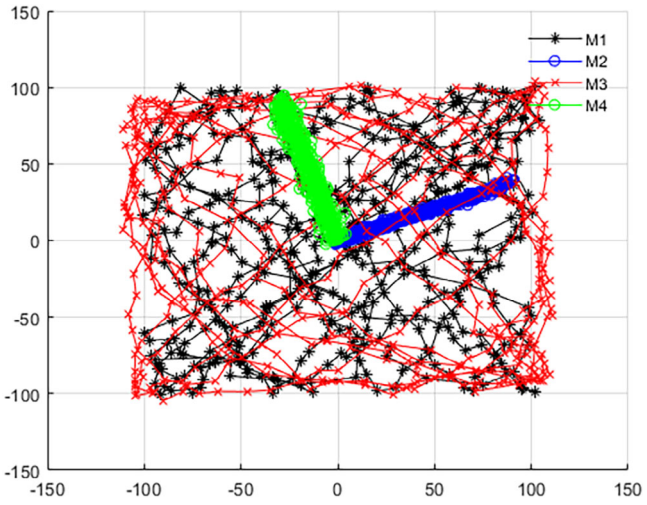

FIGURE 2 The simulated motion trajectory.

corresponding to a simulation parameter $W_{M1} = 2\pi F_{M1}$. The triangular wave has a rise phase percentage $T_{on} = 0.5$ and an amplitude $A_{M1} = 100$. The simulation is conducted over 500 steps with a step size of 0.02 s. During each simulation step, Gaussian noise with a covariance matrix of $diag[0.0001, 0.00003, 0.001]$ is added to the parameters $[W_{M1}, T_{on}, A_{M1}]$, and during observation, Gaussian noise with a covariance of 5 is introduced.

Models M_2 and M_4 engage in linear motion starting from an initial position $[x_0, y_0]$. The simulation comprises 500 steps with a step size of 0.02 s. The velocities are set to $v_x = -x_0/(500 \times 0.02)$ and $v_y = -y_0/(500 \times 0.02)$. Gaussian noise with a covariance matrix $diag[0.001, 0.001]$ is incorporated into the position and velocity parameters during each simulation step. Additionally, Gaussian noise with a covariance of 5 is introduced during observation.

For motion model M_3, a triangular wave pattern is executed along the x-axis and y-axis with a frequency $F_{M3} = 1$ Hz, corresponding to an angular velocity $W_{M3} = 2\pi F_{M3}$. The amplitude $A_{M3} = 100$, and the simulation is conducted over 500 steps with a step size of 0.02 s. Gaussian noise with a covariance matrix $diag[0.001, 0.001]$ is added to the parameters $[W_{M3}, A_{M3}]$ during each simulation step. Similar to the other models, Gaussian noise with a covariance of 5 is introduced during observation.

The IIIMME consists of a robust state estimator, an variable elliptical motion intention estimator, and a composite variable triangular wave motion intention estimator. Each estimator is designed to handle the corresponding motion intent of the tracked target.

The parameters for the variable elliptical motion intention estimator are as follows, while the predefined values for w and A are, respectively, 20% *and* 50% *different from the actual values used in* M_3:

$$\begin{aligned}\hat{x}_1(0) &= \begin{bmatrix} t_x & w_x & A_x & t_y & w_y & A_y \end{bmatrix}^T \\ &= \begin{bmatrix} 0 & \pi & 80 & 0 & \pi & 80 \end{bmatrix}^T, \\ f_p(\hat{x}_1(k)) &= \hat{x}_1(k+1) \\ &= \hat{x}_1(k) + \begin{bmatrix} 0.02 & 0 & 0 & 0.02 & 0 & 0 \end{bmatrix}^T, \\ h_p(\hat{x}_1(k)) &= \hat{z}_1(k) = \begin{bmatrix} p_x \\ p_y \end{bmatrix} = \begin{bmatrix} A_x \sin(w_x t_x) \\ A_y \sin(w_y t_y) \end{bmatrix}, \\ Q &= \begin{bmatrix} 0.001 & 0 & 0 & 0 & 0 & 0 \\ 0 & 0.01 & 0 & 0 & 0 & 0 \\ 0 & 0 & 0.1 & 0 & 0 & 0 \\ 0 & 0 & 0 & 0.001 & 0 & 0 \\ 0 & 0 & 0 & 0 & 0.01 & 0 \\ 0 & 0 & 0 & 0 & 0 & 0.1 \end{bmatrix}, \\ R &= \begin{bmatrix} 1 & 0 \\ 0 & 1 \end{bmatrix}, \alpha = 0.01, \beta = 2, \kappa = 0. \end{aligned} \tag{28}$$

Here $\hat{x}_1(k)$ is the estimated state; $\hat{z}_1(k)$ is the estimated position of the tracked target; $[t, w, A]$ are the time, angular frequency, and amplitude parameters for the sinusoidal motion; p_x and p_x are the positions of the tracked target along the X and Y axes; Q is the process noise covariance matrix; R is the observation noise covariance matrix, and α, β, κ are the tuning parameters.

The parameters for the variable composite triangular wave motion intention estimator are as follows, while the predefined values for w, A, and T_{on} are 20% *different from the actual values used in* M_1:

$$\begin{aligned}\hat{x}_2(0) &= \begin{bmatrix} t_x & w_x & A_x & T_{xon} & t_y & w_y & A_y & T_{yon} \end{bmatrix}^T \\ &= \begin{bmatrix} 0 & 1.6\pi & 120 & 0.4 & 0 & 1.6\pi & 120 & 0.4 \end{bmatrix}^T, \\ f_p(\hat{x}_2(k)) &= \hat{x}_2(k+1) \\ &= \hat{x}_2(k) + \begin{bmatrix} 0.02 & 0 & 0 & 0 & 0.02 & 0 & 0 & 0 \end{bmatrix}^T, \\ h_p(\hat{x}_2(k)) &= \hat{z}_2(k) = \begin{bmatrix} p_x \\ p_y \end{bmatrix} = \begin{bmatrix} h_{p1}(t_x, w_x, A_x, T_{xon}) \\ h_{p1}(t_y, w_y, A_y, T_{yon}) \end{bmatrix}, \end{aligned} \tag{29}$$

$$h_{p1}(t_x, w_x, A_x, T_{xon}) = \begin{cases} \frac{A_x}{T_{xon}\pi} \arcsin(\sin(w_x t_x)), & t_x \in A; \\ sign(\arcsin(\sin(w_x t_x))) & \\ \cdot (A_x + \frac{A_x T_{xon}}{1-T_{xon}}) - \frac{A_x}{(1-T_{xon})\pi} \arcsin(\sin(w_x t_x)), & t_x \in B; \\ \frac{A_x}{(1-T_{xon})\pi} \arcsin(\sin(w_x t_x)), & t_x \in C; \end{cases}$$

$$h_{p2}(t_y, w_y, A_y, T_{yon}) = \begin{cases} \frac{A_y}{T_{yon}\pi} \arcsin(\sin(w_y t_y)), & t_y \in D; \\ sign(\arcsin(\sin(w_y t_y))) & \\ \cdot (A_y + \frac{A_y T_{yon}}{1-T_{yon}}) - \frac{A_y}{(1-T_{yon})\pi} \arcsin(\sin(w_y t_y)), & t_y \in E; \\ \frac{A_y}{(1-T_{yon})\pi} \arcsin(\sin(w_y t_y)), & t_y \in F; \end{cases} \tag{30}$$

$$A = \left\{ t_x \left| \frac{2}{\pi} \arccos(\cos(w_x t_x)) < 1 \right. \right\} \cap \left\{ t_x \left| \left| \frac{2}{\pi} \arcsin(\sin(w_x t_x)) \right| \le 2T_{xon} \right. \right\};$$

$$B = \left\{ t_x \left| \frac{2}{\pi} \arccos(\cos(w_x t_x)) < 1 \right. \right\} \cap \left\{ t_x \left| \left| \frac{2}{\pi} \arcsin(\sin(w_x t_x)) \right| > 2T_{xon} \right. \right\};$$

$$C = \left\{ t_x \left| \frac{2}{\pi} \arccos(\cos(w_x t_x)) \ge 1 \right. \right\};$$

$$D = \left\{ t_y \left| \frac{2}{\pi} \arccos(\cos(w_y t_y)) < 1 \right. \right\} \cap \left\{ t_y \left| \left| \frac{2}{\pi} \arcsin(\sin(w_y t_y)) \right| \le 2T_{yon} \right. \right\};$$

$$E = \left\{ t_y \left| \frac{2}{\pi} \arccos(\cos(w_y t_y)) < 1 \right. \right\} \cap \left\{ t_y \left| \left| \frac{2}{\pi} \arcsin(\sin(w_y t_y)) \right| > 2T_{yon} \right. \right\};$$

$$F = \left\{ t_y \left| \frac{2}{\pi} \arccos(\cos(w_y t_y)) \ge 1 \right. \right\}; \quad (31)$$

$$Q = \begin{bmatrix} 0.001 & 0 & 0 & 0 & 0 & 0 \\ 0 & 0.01 & 0 & 0 & 0 & 0 \\ 0 & 0 & 0.1 & 0 & 0 & 0 \\ 0 & 0 & 0 & 0.001 & 0 & 0 \\ 0 & 0 & 0 & 0 & 0.01 & 0 \\ 0 & 0 & 0 & 0 & 0 & 0.1 \end{bmatrix},$$

$$R = \begin{bmatrix} 1 & 0 \\ 0 & 1 \end{bmatrix}, \alpha = 0.01, \beta = 2, \kappa = 0. \quad (32)$$

The parameters for the robust state estimator are as follows:

$$F = \begin{bmatrix} 1 & 0.02 & 0 & 0 \\ 0 & 1 & 0 & 0 \\ 0 & 0 & 1 & 0.02 \\ 0 & 0 & 0 & 1 \end{bmatrix}, G = \begin{bmatrix} 1 & 0.02 & 0 & 0 \\ 0 & 1 & 0 & 0 \\ 0 & 0 & 1 & 0.02 \\ 0 & 0 & 0 & 1 \end{bmatrix},$$

$$H = \begin{bmatrix} 1 & 0 & 0 & 0 \\ 0 & 0 & 1 & 0 \end{bmatrix}, Q = \begin{bmatrix} 1 & 0 & 0 & 0 \\ 0 & 1 & 0 & 0 \\ 0 & 0 & 1 & 0 \\ 0 & 0 & 0 & 1 \end{bmatrix},$$

$$R_0 = \begin{bmatrix} 1 & 0 \\ 0 & 1 \end{bmatrix}, x_0 = \begin{bmatrix} 0 \\ 1 \\ 0 \\ 1 \end{bmatrix}, P_0 = \begin{bmatrix} 1 & 0 & 0 & 0 \\ 0 & 1 & 0 & 0 \\ 0 & 0 & 1 & 0 \\ 0 & 0 & 0 & 1 \end{bmatrix},$$

$$E_f = \begin{bmatrix} 0 & 0.1 & 0 & 0.1 \end{bmatrix}, E_f = \begin{bmatrix} 0 & 0.1 & 0 & 0.1 \end{bmatrix},$$

$$M = \begin{bmatrix} 0.1 & 0 & 0.1 & 0 \end{bmatrix}^T, \quad (33)$$

where $\hat{x}_2(k)$ is the estimated state; $\hat{\tilde{x}}_2(k)$ is the estimated position of the tracked target; $[t, w, A, T_{on}]$ are the time, angular frequency, amplitude, and rise ratio parameters for the triangular wave motion; p_x and p_y are the positions of the tracked target along the X and Y axes; Q is the process noise covariance matrix; R is the observation noise covariance matrix; and α, β, κ are the tuning parameters.

The other parameters used in the IIIMME are as follows:

$$\Gamma = \begin{bmatrix} 0.9 & 0.05 & 0.05 \\ 0.05 & 0.9 & 0.05 \\ 0.05 & 0.05 & 0.9 \end{bmatrix}, \mu_j = \begin{bmatrix} 0.4 \\ 0.3 \\ 0.3 \end{bmatrix}, \hat{\tilde{x}}(0) = \begin{bmatrix} 0.1 \\ 0.1 \end{bmatrix}. \quad (34)$$

For the trajectory in Figure 2, the study conducted simultaneous estimation using multiple estimation methods and compared their performance in terms of estimation accuracy. These estimation methods include the proposed IIIMME; the classical IMM estimation method (IMMC), which uses precise initial values and traditional model in the form of (4); the robust estimation method (RE); the separate variable elliptical wave motion intention estimator (UKE1); and the separate variable composite triangular wave motion intention estimator (UKE2). The estimation errors of the tracked target on the X-axis by five estimators are presented in Figure 3.

From Figure 3, it can be observed that the separate intention estimators (UKE1 and UKE2) achieve good estimation results during their respective intent phases (M_1 or M_3) but show lower accuracy in other cases (M_2 and M_4). The newly proposed IIIMME demonstrates significantly better performance compared to others, with the highest accuracy. The IMMC and the RE exhibit slightly lower accuracy, but their estimation results remain usable throughout the entire trajectory without significant degradation. To provide a clearer comparison of the strengths and weaknesses of different estimation methods, the accumulated estimation error results for the different estimators are plotted in Figure 4. The accumulated estimation error refers to the distance between the true position of the tracked target and its estimated position.

It can be observed that the UKE1 and UKE2 exhibit a low error accumulation rate during their respective adaptation phases, which is similar to the performance of the IIIMME and better than the IMMC and the RE. The proposed IIIMME demonstrates the best estimation accuracy throughout all phases, estimates much better than the traditional IMM designing method, and confirms the stability and effectiveness of IIIMME.

6.2 | Experiment

To further validate the effectiveness of the proposed method, the algorithms of the aforementioned estimators were

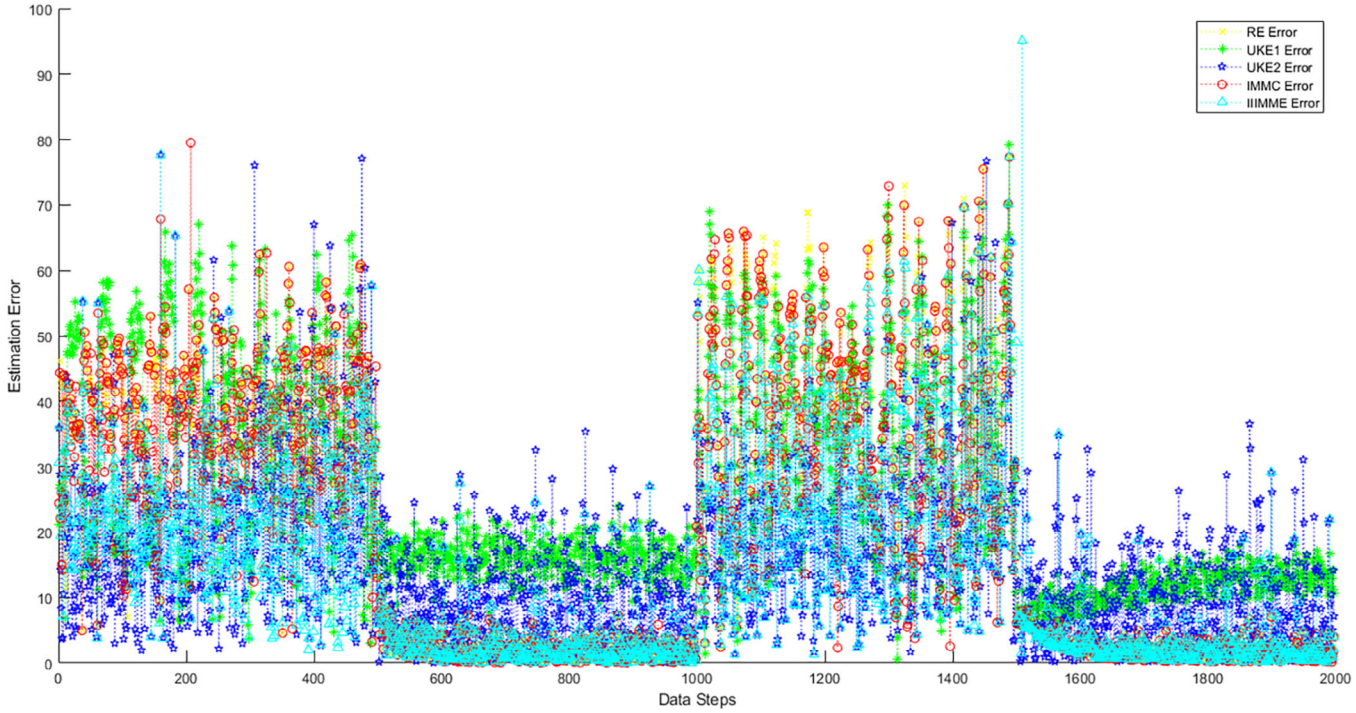

FIGURE 3 The estimation error of different estimators.

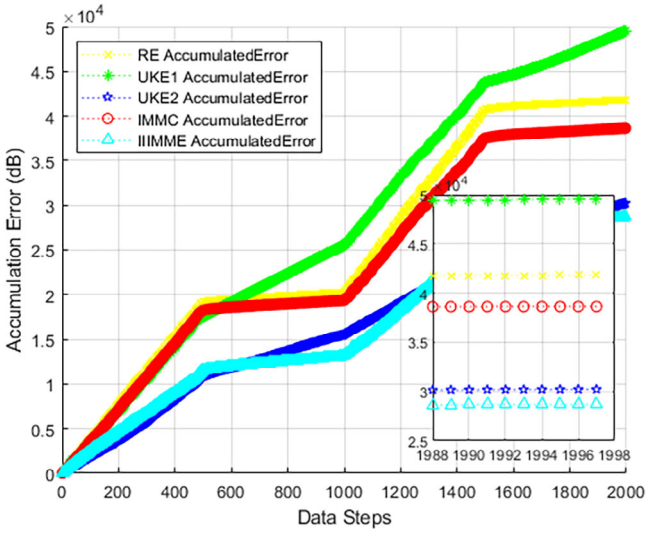

FIGURE 4 The accumulated estimation error of different estimators.

implemented as C language programme and the experimental verification was conducted on a dual-reflector mirror experimental platform. The platform consists of four main devices, as shown in Figure 5.

These devices include a laser generator for simulating the position of the tracked target, a disturbance mirror for simulating the motion of the tracked target, a validation mirror for verifying the control and estimation algorithms, and a CCD camera for simulating the image sensor of the photoelectric tracking system. The disturbance mirror utilizes four voice coil motors and matching eddy current sensors to form position signal feedback. After testing the frequency response of the motors, a controller is designed using the pole-zero cancellation method to form a closed-loop control. The validation mirror, based on the eddy current sensor's position inner loop, uses the CCD camera signal as feedback to test the inner loop's frequency response. The controller is then designed based on this frequency response and pole-zero cancellation method to form a dual closed-loop. The prediction algorithm is applied to the feedback path of the CCD camera signal to compensate for noise and delay.

During the experimental process, this study sent open-loop sine signals with different phases to the four voice coil motor drivers of the disturbance mirror. Due to friction dead zone and unbalanced torque effects, the mirror will undergo distorted sinusoidal motion in both the horizontal and vertical axes. When the beam is transmitted to the CCD camera, noise will be present in the observations due to the uneven medium introduced in the optical path and the camera resolution. Since the camera's signal output frequency is 50 Hz and it requires 0.04 s for image signal acquisition and processing, the video signal obtained by the controller has a two-frame delay. In other words, the motion trajectory data input to the controller is a distorted sinusoidal wave with delay and noise. The designed state estimator in this study will be used to remove observation noise, perform a two-step prediction to compensate for camera delay, and restore the true motion trajectory.

In the experiment, the estimation accuracy of the five state estimators, that is, IIIMME, IMMC, RE, UKE1, UKE2, were also compared with identical parameters in (33), (28), (29) and (34). The estimation results are as shown in Figures 6 and 7. It

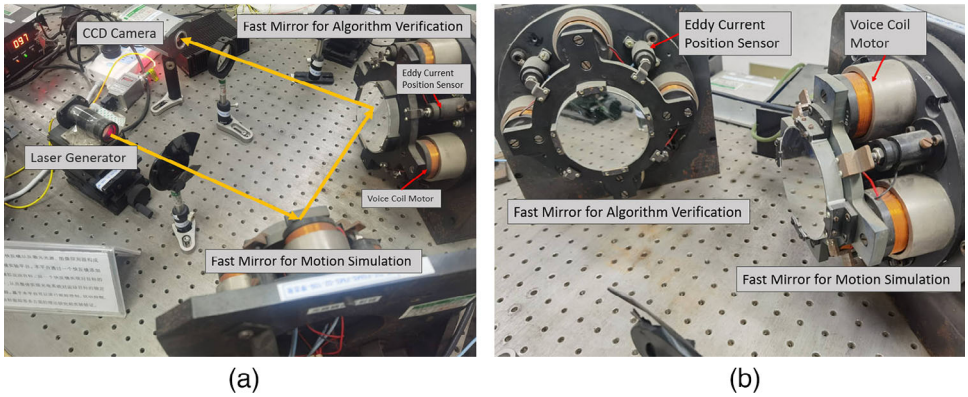

FIGURE 5 Dual-reflection mirror experimental platform.

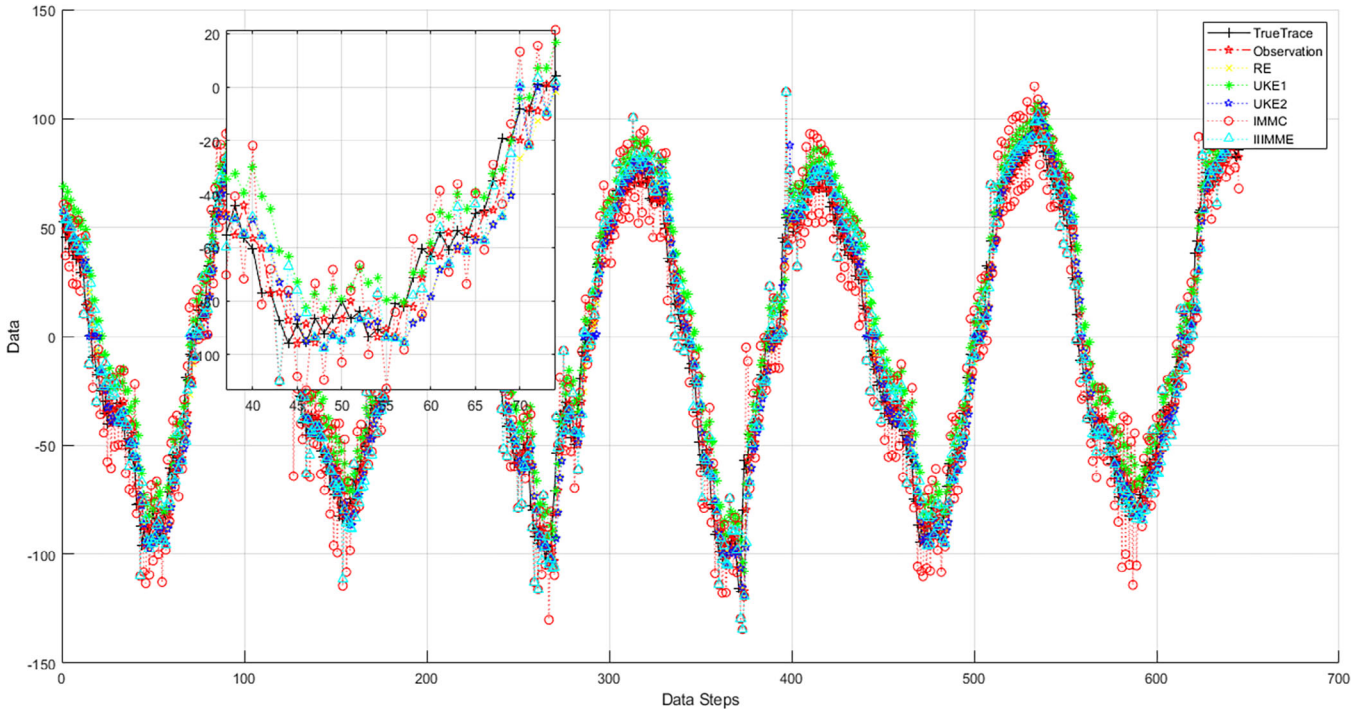

FIGURE 6 The observed trace and two step prediction results of differnt estimators.

can be observed that the newly proposed estimation method in this study exhibits the best estimation accuracy in the experiment, demonstrating good adaptability and stability. Due to the influence of non-linear friction forces, the inflection points of the spot motion trajectory are relatively sharp, and the curved motion approaches a straight line. Therefore, UKE1 achieves estimation accuracy second only to IIIMME. Following that are the estimation results of IMMC and RE, which are still usable but noticeably weaker than the new method. The least effective is UKE2, indicating a significant decrease in estimation performance when the intent model is incompatible with the actual trajectory. This also underscores the importance of including RE in the IIIMME method, ensuring that when a completely new motion pattern arises, IIIMME can degrade to RE and continue functioning.

7 | CONCLUSION

Traditional methods for target state estimation commonly rely on using the external physical quantities of the tracked target, such as position and velocity, as the estimated states. However, when dealing with non-cooperative manoeuvering targets, this approach faces challenges in achieving accurate estimation and prediction. In this study, we propose using parameters related to the target's motion intention in our estimators, as intention represents a stable state that enhances the accuracy of position estimation and facilitates medium-to-long-term prediction. Specifically, we introduced a method that using modified IMM approach to combine multiple specific intention estimators and a generic robust estimator to achieve more accurate manoeuvering target state estimation.

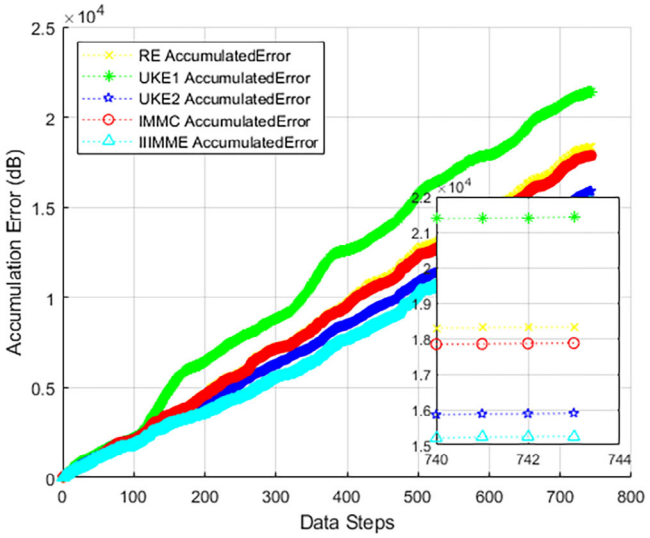

FIGURE 7 The accumulated estimation error of different estimators.

There are several areas in this research that can be further improved. First, this estimator requires excellent trajectory clustering and representation techniques to achieve better matching with motion models, which is waiting to explore. Second, the interactive mechanism for different motion intentions can be explored further to enhance its performance. Third, it would be beneficial to investigate and apply other non-linear estimation methods that are faster and more accurate than the UKE method.

We believe that the new approach presented here can effectively enhance the position prediction capability of optical tracking systems for manoeuvering targets. The estimation method based on intention inference holds promise for more effective medium-to-long-term prediction.

AUTHOR CONTRIBUTIONS

Minxing Sun: Conceptualization; data curation; formal analysis; methodology; resources; software; validation; visualization; writing—original draft; writing—review and editing. **Huabo Liu**: Conceptualization; investigation; supervision; writing—review and editing. **Qianwen Duan**: Conceptualization; data curation; formal analysis; resources; writing—review and editing. **Junzhe Wang**: Data curation; formal analysis; validation. **Yao Mao**: Investigation; methodology; project administration; resources; supervision; writing—review and editing. **Qiliang Bao**: Project administration; resources; supervision; validation.

CONFLICT OF INTEREST STATEMENT

The authors declare no potential conflict of interests.

DATA AVAILABILITY STATEMENT

Data is sharing not applicable as no new data were generated; the article describes entirely theoretical research.

ORCID

Yao Mao https://orcid.org/0000-0003-1785-2018

REFERENCES

1. Wang, F., Wang, R., Xie, M., Liu, P., Jing, F., Liu, B.: Tracking control Scheme for photoelectric tracking platform with predictor-structure ESO. In: 2021 International Conference on Machine Learning and Intelligent Systems Engineering (MLISE), pp. 117–125. IEEE, Piscataway, NJ (2021)
2. Ghommam, J., Fethalla, N., Saad, M.: Quadrotor circumnavigation of an unknown moving target using camera vision-based measurements. IET Control Theory Appl. 10(15), 1874–1887 (2016)
3. Kaymak, Y., Rojas-Cessa, R., Feng, J., Ansari, N., Zhou, M., Zhang, T.: A survey on acquisition, tracking, and pointing mechanisms for mobile free-space optical communications. IEEE Commun. Surv. Tutorials 20(2), 1104–1123 (2018)
4. Zhijun, L., Yao, M., Bo, Q., Xi, Z., Qiong, L., Qian, Z.: Research on control technology of single detection based on position correction in quantum optical communication. Opto-Electron. Eng. 49(3), 210311 (2022)
5. Sorriento, A., Porfido, M.B., Mazzoleni, S., Calvosa, G., Tenucci, M., Ciuti, G., et al.: Optical and electromagnetic tracking systems for biomedical applications: a critical review on potentialities and limitations. IEEE Rev. Biomed. Eng. 13, 212–232 (2020)
6. Yu, N., Genevet, P., Aieta, F., Kats, M.A., Blanchard, R., Aoust, G., et al.: Flat optics: controlling wavefronts with optical antenna metasurfaces. IEEE J. Sel. Top. Quantum Electron. 19(3), 4700423 (2013)
7. Wojke, N., Bewley, A., Paulus, D.: Simple online and realtime tracking with a deep association metric. In: 2017 24th IEEE International Conference on Image Processing (ICIP), pp. 3645–3649. IEEE, New York (2017)
8. Nguyen, X.M., Lee, J.Y., Lee, S.T., Hong, S.K.: Target state estimation for UAV's target tracking and precision landing control: algorithm and verification system. In: 21st International Conference on Control, Automation and Systems (ICCAS), pp. 173–177. IEEE, New York (2021)
9. Wenqiang, X., Qiunong, H., Qianwen, D., Xi, Z., Jiuqiang, D., Yao, M.: 'Equivalent acceleration feedforward based on sensor optimization and robust prediction'. Opto-Electron. Eng. 48(11), 210153 (2021)
10. Zhao, T., Tong, W., Mao, Y.: Hybrid nonsingleton fuzzy strong tracking Kalman filtering for high precision photoelectric tracking system. IEEE Trans. Ind. Inf. 19(3), 2395–2408 (2023)
11. Ren, W., Mao, Y., Li, Z., Ren, G.: Error-based feedforward control for photoelectric tracking system. In: Chinese Automation Congress (CAC), pp. 460–465. IEEE, New York (2019)
12. Deng, J., Xue, W., Liang, W., Zhou, X., Mao, Y.: On adjustable and lossless suppression to disturbances and uncertainties for nonminimum-phase laser pointing system. ISA Trans. 136, 727–741 (2023)
13. Ren, W., Luo, Y., He, Q., Zhou, X., Deng, C., Mao, Y., et al.: Stabilization control of electro-optical tracking system with fiber-optic gyroscope based on modified Smith predictor control scheme. IEEE Sens. J. 18(19), 8172–8178 (2018)
14. Ding, L., Wang, H.N., Guan, Z.H., Chen, J.: Tracking under additive white Gaussian noise effect. IET Control Theory Appl. 4(11), 2471–2478 (2010)
15. Teets, D., Whitehead, K.: The discovery of Ceres: how Gauss became famous. Math. Mag. 72(2), 83–93 (1999)
16. Wiener, N.: The linear predictor for a single time series. In: Extrapolation, Interpolation, and Smoothing of Stationary Time Series: With Engineering Applications, pp. 56–80. MIT Press, Cambridge, MA (1964)
17. Kalman, R.E.: A new approach to linear filtering and prediction problems. J. Basic Eng. 82(1), 35–45 (1960)
18. Zames, G.: Feedback and optimal sensitivity: Model reference transformations, multiplicative seminorms, and approximate inverses. IEEE Trans. Autom. Control 26(2), 301–320 (1981)
19. Zhou, B., Zheng, W.X., Fu, Y.M., Duan, G.R.: H-infinity filtering for linear continuous-time systems subject to sensor non-linearities. IET Control Theory Appl. 5(16), 1925–1937 (2011)
20. Sayed, A.H.: A framework for state-space estimation with uncertain models. IEEE Trans. Autom. Control 46(7), 998–1013 (2001)
21. Li, Z., Sun, M., Duan, Q., Mao, Y.: Robust state estimation for uncertain discrete linear systems with delayed measurements. Mathematics 10(9), 1365 (2022)
22. Sun, M., Mao, Y., Liu, H.: A robust state estimator with adaptive factor. IEEE Access 8, 144514–144521 (2020)

23. Julier, S.J., Uhlmann, J.K.: A new extension of the Kalman filter to nonlinear systems. In: SPIE Proceedings, vol. 3068, pp. 182–193. Society of Photo-Optical Instrumentation Engineers, Bellingham, WA (1997)
24. Arasaratnam, I., Haykin, S.: Cubature Kalman filters. IEEE Trans. Autom. Control 54(6), 1254–1269 (2009)
25. Ma, K., Xu, L., Fan, H.: Unscented Kalman filtering for target tracking systems with packet dropout compensation. IET Control Theory Appl. 13(12), 1901–1908 (2019)
26. Wu, C.H., Wei, C.C., Su, D.C., Chang, M.H., Ho, J.M.: Travel time prediction with support vector regression. In: 6th IEEE International Conference on Intelligent Transportation Systems, pp. 1438–1442. IEEE, New York (2003)
27. Messaoud, K., Yahiaoui, I., Verroust-Blondet, A., Nashashibi, F.: Relational recurrent neural networks for vehicle trajectory prediction. In: IEEE Intelligent Transportation Systems Conference (IEEE-ITSC), pp. 1813–1818. IEEE, New York (2019)
28. Schoelkopf, B., Locatello, F., Bauer, S., Ke, N.R., Kalchbrenner, N., Goyal, A., et al.: Toward causal representation learning. Proc. IEEE 109(5), 612–634 (2021)
29. Doucet, A., Gordon, N.J., Krishnamurthy, V.: Particle filters for state estimation of jump Markov linear systems. IEEE Trans. Signal Process. 49(3), (2001)
30. Yang, X., Zhao, X.: Mixed particle filtering for maneuvering target tracking in clutter. In: Mohammadian, M. (ed.) International Conference on Computational Intelligence for Modelling, Control and Automation, pp. 557–562. IEEE, New York (2008)
31. Truong, T.Q.S.: Exploration of adaptive filters for target tracking in the presence of model uncertainty. In: 2010 Sixth International Conference on Intelligent Sensors, Sensor Networks and Information Processing, pp. 1–6. IEEE, Piscataway, NJ (2010)
32. Blom, H., Barshalom, Y.: The interacting multiple model algorithm for systems with Markovian switching coefficients. IEEE Trans. Autom. Control 33(8), 780–783 (1988)
33. Fu, X., Jia, Y., Du, J., Yu, F.: New interacting multiple model algorithms for the tracking of the manoeuvring target. IET Control Theory Appl. 4(10), 2184–2194 (2010)
34. Lim, J., Kim, H.S., Park, H.M.: Interactive-multiple-model algorithm based on Minimax particle filtering. IEEE Signal Process Lett. 27, 36–40 (2020)
35. Zeng, Y., Lu, W., Yu, B., Tao, S., Zhou, H., Chen, Y.: Improved IMM algorithm based on support vector regression for UAV tracking. J. Syst. Eng. Electron. 33(4), 867–876 (2022)
36. Zhou, G., Zhu, B., Ye, X.: Switch-constrained multiple-model algorithm for maneuvering target tracking. IEEE Trans. Aerosp. Electron. Syst. 59(4), 4414–4433 (2023)
37. Hernandez, M., Farina, A.: PCRB and IMM for target tracking in the presence of specular multipath. IEEE Trans. Aerosp. Electron. Syst. 56(3), 2437–2449 (2020)
38. Han, L., Xie, A., Ren, Z., Bernstein, D.S.: Maneuvering target tracking with unknown acceleration using retrospective-cost-based adaptive input and state estimation. In: Zhao, Q., Liu, S. (eds.) 34th Chinese Control Conference (CCC), pp. 5029–5034. IEEE, New York (2015)
39. Doyle, J.: Robust and optimal control. In: Proceedings of 35th IEEE Conference on Decision and Control, vol. 2, pp. 1595–1598. IEEE, Piscataway, NJ (1996)
40. He, Q., Luo, Y., Mao, Y., Zhou, X.: An acceleration feed-forward control method based on fusion of model output and sensor data. Sens. Actuators A-Phys. 284, 186–193 (2018)

How to cite this article: Sun, M., Liu, H., Duan, Q., Wang, J., Mao, Y., Bao, Q.: Intention inference-based interacting multiple model estimator in photoelectric tracking. IET Control Theory Appl. 18, 1210–1222 (2024). https://doi.org/10.1049/cth2.12657